Applied Catalysis B: Environmental 88 (2009) 490–496

Contents lists available at ScienceDirect

Applied Catalysis B: Environmental

journal homepage: www.elsevier.com/locate/apcatb

Steady-state isotopic transient kinetic analysis of steam reforming of methanol over Cu-based catalysts

Joan Papavasiliou [a,b], George Avgouropoulos [a], Theophilos Ioannides [a,*]

[a] Foundation for Research and Technology-Hellas (FORTH), Institute of Chemical Engineering and High Temperature Chemical Processes (ICE-HT), P.O. Box 1414, GR-26500 Patras, Greece
[b] Department of Chemical Engineering, University of Patras, GR-26500 Patras, Greece

ARTICLE INFO

Article history:
Received 7 August 2008
Received in revised form 13 October 2008
Accepted 18 October 2008
Available online 6 November 2008

Keywords:
SSITKA
Steam reforming
Methanol
Copper
Ceria
Manganese

ABSTRACT

Mechanistic aspects of steam reforming of methanol were studied via steady-state isotopic transient kinetic analysis over three copper-based catalysts, namely combustion-synthesized Cu-Ce-O and Cu-Mn-O, and commercial Cu-ZnO-Al_2O_3. The "C-path" and "O-path" for the production of CO_2 via steam reforming of methanol was analysed with the following step changes in the feed: $^{12}CH_3OH/H_2O/Ar/He \rightarrow {}^{13}CH_3OH/H_2O/He$ and $CH_3OH/H_2{}^{16}O/Ar/He \rightarrow CH_3OH/H_2{}^{16}O/H_2{}^{18}O/He$. The presence of $CH_3{}^{18}OH$ in the products after the switch to ^{18}O-labeled water indicates that a major path of the reaction is the one involving a methyl formate intermediate. This appears to be the main path over the Cu-Mn-O catalyst, while parallel paths via dioxomethylene and methyl formate intermediates appear to be operative over Cu-Ce-O and Cu-ZnO-Al_2O_3 catalysts.

1. Introduction

Steam Reforming of Methanol (SRM), is a promising process of hydrogen production on-board for use in fuel cells.

$$CH_3OH + H_2O \rightarrow 3H_2 + CO_2, \quad \Delta H = +49.4\,kJ\,mol^{-1} \qquad (1)$$

Copper-based catalysts have been identified as the most effective for the SRM reaction and thus are the subject of intensive research [1–6]. A number of different mechanisms describing the SRM over Cu-based catalysts have been proposed in the literature and arguments exist about the mechanism of CO by-product formation and the reaction route involving a methyl formate intermediate [7–11].

Steady-state isotopic transient kinetic analysis (SSITKA) has long been documented and widely accepted as one of the most powerful techniques to elucidate in a precise way mechanisms of heterogeneous reactions [12–14]. Important aspects of this technique, the necessary flow system and the analysis of the results have been discussed thoroughly by Shannon and Goodwin [15,16] and Efstathiou and Verykios [17]. Many studies have been reported on application of SSITKA techniques over a wide range of surface-catalyzed reactions including water-gas shift (WGS) [18], ammonia synthesis [19], combustion [20] and reforming of methane [21], methanol synthesis [22], and others.

In the present study, SSITKA-Mass Spectrometry experiments were performed in order to study mechanistic aspects of the steam reforming of methanol over three selected Cu-based catalysts: Cu-Mn-O and Cu-Ce-O catalysts, prepared by the urea-nitrate combustion method, and a commercial Cu-ZnO-Al_2O_3 catalyst. Up to now, several mechanistic studies on the SRM reaction have been carried out with in-situ DRIFTS techniques [8,10,11,23]. This paper presents the first –to our knowledge- investigation of the SRM reaction over copper-based catalysts with the SSITKA technique.

2. Experimental

2.1. Catalysts

Selected Cu-Mn-O and Cu-Ce-O catalysts were prepared via the urea-nitrate combustion method. Details of synthesis and characterization procedures have been reported elsewhere [3,24,25]. The molar ratios of urea/nitrate = 4.17, Cu/(Cu + Mn) = 0.30 and Cu/(Cu + Ce) = 0.15, previously determined to yield catalysts with optimal performance in the SRM reaction, were used. The catalytic activity of Cu-Mn-O catalyst was found to be comparable to that of a commercial Cu-ZnO-Al_2O_3 catalyst, which is also studied in the present work.

* Corresponding author. Tel.: +30 2610 965264; fax: +30 2610 965223.
E-mail address: theo@iceht.forth.gr (T. Ioannides).

0926-3373/$ – see front matter © 2008 Elsevier B.V. All rights reserved.
doi:10.1016/j.apcatb.2008.10.018

2.2. Procedure

SSITKA experiments were done with the following gas mixtures, which were prepared in the laboratory: 2% H_2O/He and 2% CH_3OH/He, using 3D water and CH_3OH (Merck, 99.9% purity) and the isotopic gas mixtures 1% $H_2{}^{16}O$/1% $H_2{}^{18}O$/He and 2% $^{13}CH_3OH$/He, using the isotopes $^{13}CH_3OH$ (99 at% ^{13}C, Isotec) and $H_2{}^{18}O$ (97 at% ^{18}O, Isotec). SSITKA experiments concerning the study of the "carbon-path, C-path" of reaction, involved the switch: $^{12}CH_3OH/H_2O/He/Ar \rightarrow {}^{13}CH_3OH/H_2O/He$, while those concerning the "oxygen-path, O-path" of the reaction, involved the switch: $CH_3OH/H_2{}^{16}O/He/Ar \rightarrow CH_3OH/H_2{}^{16}O/H_2{}^{18}O/He$. Switching between the two feedstreams was done with the use of a 4-port valve, without perturbing the course of reaction. Argon, present as an inert tracer, was removed from the feedstream during the switch, in order to determine gas-phase holdup for the reactor system. Its concentration (0.5%) was small enough in order not to perturb the reaction during the switch. The initial time of the transient response, t_0, was typically taken as the beginning of Ar transient response. Mass flow controllers for every component in the feed, provide two feedstreams with identical composition (0.5% MeOH, H_2O/MeOH = 1.5) and total flow (F_T = 40 $cm^3\ min^{-1}$ STP). A bypass of the reactor and a second 4-port valve allow checking the exact composition of the reactor inlet and correcting if necessary. All experiments were performed in a quartz tube reactor (4 mm i.d., 6 mm o.d., length 30 cm) at 190 °C and atmospheric pressure. A PID control thermocouple was enclosed in a 3 mm o.d. quartz thermowell placed coaxially into the reactor tube and inserted into the catalyst bed. The mass of the catalysts (in the form of powder with particle size in the range 90 μm < d_p < 180 μm; catalyst bed height: 2–4 mm) was adjusted so as to keep the methanol conversion below 20%.

All reactants, products and possible intermediate species, as well as their corresponding isotopic labelled species were continuously monitored by an on-line mass spectrometer (Omnistar/Pfeiffer Vacuum). The only detected, carbon-containing product was carbon dioxide in all cases. Under the conditions of the SSITKA experiments (low temperature, low methanol conversion), CO formation was negligible, in agreement with results obtained under steady-state catalytic tests [24,25].

3. Results and discussion

3.1. Investigation of "C-path"

Fig. 1 presents the normalized responses of Ar, $^{12}CO_2$ and $^{13}CO_2$ after the switch: $^{12}CH_3OH/H_2O/Ar/He \rightarrow {}^{13}CH_3OH/H_2O/He$ over the Cu-Ce-O catalyst. Normalized response curves of all reactants and products during the isotopic switch over the Cu-Ce-O catalyst are shown in Fig. 2. Methanol conversion under the standard experimental reaction conditions was 11%. The overall mean surface-residence time, "τ", of all adsorbed intermediate species which contain carbon, participate in the mechanistic C-path and lead to CO_2 formation, can be calculated through Eq. (2):

$$\bar{\tau}^{CO_2} = \bar{\tau}_m^{CO_2} - \bar{\tau}_g^{Ar} \quad (2)$$

where $\bar{\tau}_m^{CO_2}$ (measured) and $\bar{\tau}_g^{Ar}$ (gas-phase hold up) refer to the measured response curves of the species and can be obtained from integration of the normalized responses of $^{12}CO_2$ and Ar, respectively. For the $Cu_{0.15}Ce_{0.85}$ catalyst, this quantity is equivalent to the crosshatched area in Fig. 1 and is equal to 749 s.

The $^{12}CO_2$ and $^{13}CO_2$ responses in Fig. 1 reflect the transient incorporation of ^{13}C-atoms into the ^{12}C-containing intermediate species present under steady state conditions, which participate in the formation of carbon dioxide. Eventually, a new steady state will be achieved, at which the only carbon dioxide product observed will be $^{13}CO_2$. In the experiment depicted in Fig.1, times longer than 37 min are required in order to achieve this new steady state and completely replace all ^{12}C-atoms with ^{13}C-atoms, in the various carbon-containing intermediate species which lead to CO_2 formation. It has been reported in the literature that this new steady state is usually achieved in a time window between 2 and 10 min for various types of reactions [12,18,21,20]. Nevertheless, it is not the first time that such long transition times are reported. Suprun et al. [26] investigated the role of water in the reaction mechanism of the selective oxidation of 1-butene on VO_x–TiO_2 by SSITKA, and found that ~17 min were required in order for the non-labelled product to drop down to 10% of its initial concentration. In our case, ~28 min are necessary for the $^{12}CO_2$ level to drop down to 10% of its original value. Rozovskii [27] has reported that methanol, dimethyl ether and methyl formate synthesis as well as methanol steam reforming over Cu-based catalysts are systems which contain species (reactants or products) that are strongly-

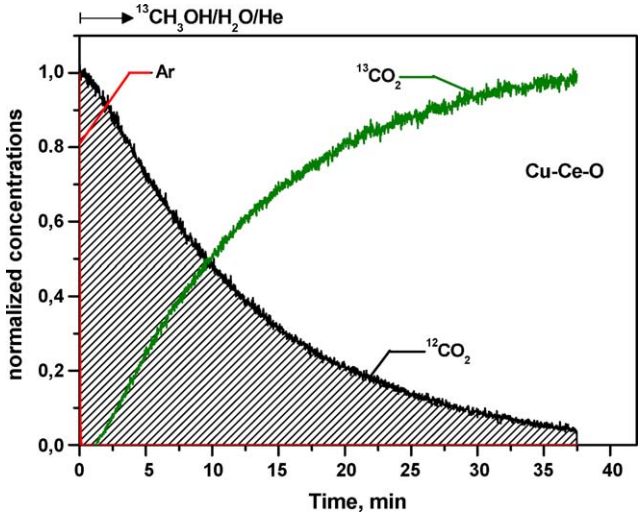

Fig. 1. Normalized responses of Ar and carbon dioxide after the switch: $^{12}CH_3OH/H_2O/Ar/He \rightarrow {}^{13}CH_3OH/H_2O/He$. Cu-Ce-O catalyst at 463 K.

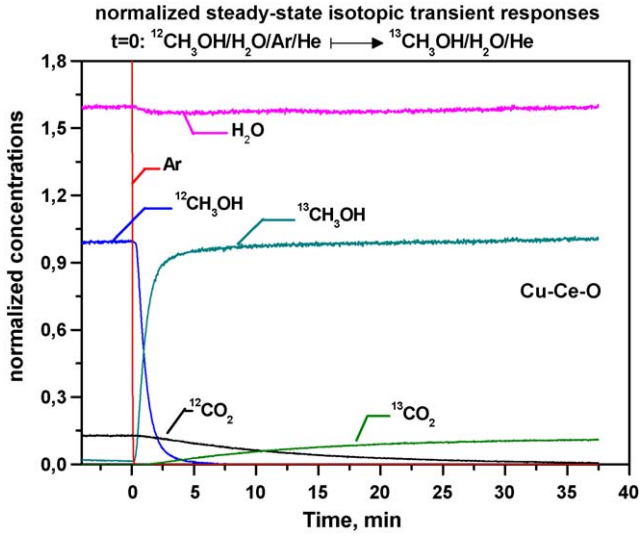

Fig. 2. Response curves of reactants and products according to the gas delivery sequence: $^{12}CH_3OH/H_2O/Ar/He \rightarrow {}^{13}CH_3OH/H_2O/He$. Cu-Ce-O catalyst at 463 K (all curves normalized with respect to methanol).

'irreversibly' adsorbed on the catalyst. He defines the term 'irreversibly' in the sense that the characteristic times of adsorption of a given species are much longer than the characteristic time of a catalytic reaction.

The concentration (μmol g^{-1}) of C-containing intermediate species which participate in the formation of carbon dioxide via the steam reforming of methanol can be calculated from the following equation:

$$\bar{N}^{CO_2}\,(\mu\text{mol CO}_2\,g_{cat}^{-1}) = \left(\frac{F_T}{W}\right)\left[\int_0^t (y^{^{12}CO_2} - y^{Ar})dt\right] \quad (3)$$

where y^i is the molar fraction (ppm) of the gas phase species i, F_T is the total molar flow rate (mol min^{-1}) at the reactor outlet, W is the catalyst mass (g).

The concentration of adsorbed intermediate species which lead to the formation of CO_2 is equal to 235 μmol g^{-1} for the Cu-Ce-O catalyst. According to Shannon and Goodwin [15,16] the overall reaction rate at steady state, regardless of the underlying kinetics or mechanism, can be obtained using the relationship:

$$\bar{r}^{CO_2} = \frac{\bar{N}^{CO_2}}{\bar{\tau}^{CO_2}} \quad (4)$$

Using Eq. 4, that overall reaction rate of the SRM reaction over the Cu-Ce-O catalyst is found to be 0.31 μmol g_{cat}^{-1} s^{-1}.

SSITKA analysis can provide information relevant to the reaction mechanism. Such information can be obtained by the semi-logarithmic representation of the molar fraction of a reaction product versus time. The shape of the curve is characteristic of the type of mechanism responsible for its formation. More specifically, the resulting profile reflects the heterogeneity of surface intermediates (in the case of a mechanism which proceeds via a buffer step, parallel routes or consecutive pools) or the homogeneity (in the case of one pool mechanism) [12,15,19,28]. In each case, the semi-logarithmic plot of the molar fraction of product species against time has a different shape, as described by Burch et al. [12]. The semi-logarithmic plot of the molar fraction of CO_2, $\ln(y^{CO_2})$ versus time, in the case of the Cu-Ce-O catalyst, is presented in Fig. 3. The curve appears to be slightly convex in the first few minutes and straightens out at longer times. A straight line in the semi-logarithmic plot corresponds to either a direct mechanism (whose plot is straight line) or a combination of parallel reactions and reactions in series, while a convex shape corresponds to a consecutive mechanism [12,15,19,28]. In view of these observations, a straightforward allocation of a reaction path is not possible.

Fig. 4 shows gas phase responses of $^{12}CO_2$, $^{13}CO_2$ and Ar species at the reactor outlet after the switch $^{12}CH_3OH/H_2O/He/Ar \rightarrow {}^{13}CH_3OH/H_2O/He$ over the Cu-Mn-O catalyst. The steady-state methanol conversion was 20%. The overall mean surface residence time, "τ", of all adsorbed intermediate species which contain carbon, participate in the mechanistic C-path and lead to CO_2 formation, is found to be 107 s. The concentration of these species on the catalyst surface and the corresponding CO_2 production rate were 361 μmol g_{cat}^{-1} and 3.38 μmol g_{cat}^{-1} s^{-1}, respectively. As it can be seen in Fig. 4, the complete replacement of all $^{12}CO_2$ by $^{13}CO_2$ takes place after ~30 min, as in the case of Cu-Ce-O catalyst. Nevertheless, the response curves of CO_2 as well as of CH_3OH, have different shape, as it can be seen in Fig. 5. The semi-logarithmic plot of the molar fraction of CO_2 produced, $\ln(y^{CO_2})$ versus time in the case of Cu-Mn-O catalyst (Fig. 3), has a clear concave shape during the first ~15 min which is indicative of a parallel mechanism or a mechanism with the presence of a buffer step [12].

Fig. 6 presents the transient normalized response curves of $^{12}CO_2$, $^{13}CO_2$ and Ar obtained after the isotopic switch over the commercial Cu-ZnO-Al_2O_3 catalyst at 190 °C (MeOH conversion = 20%). Based on the crosshatched areas in Fig. 6 the overall mean surface residence time of all of the adsorbed intermediate species which lead to CO_2 formation, is found to be 141 s, while the concentration of these species on the catalyst surface and the CO_2 production rate were equal to 386 μmol g_{cat}^{-1} and 2.74 μmol g_{cat}^{-1} s^{-1}, respectively. The time needed for the achievement of the new steady-state is more than 30 min. Normalized response curves of carbon dioxide and methanol during the isotopic switch over the Cu-ZnO-Al_2O_3 catalyst (not shown) are similar to those of the Cu-Mn-O catalyst shown in Fig. 5.

The semi-logarithmic plot of the molar fraction of CO_2 produced from the steam reforming of methanol over the Cu-ZnO-Al_2O_3 commercial catalyst versus time has a complex shape, as shown in Fig. 3. During the first ~10 min the curve is concave, as it was in the case of Cu-Mn-O catalyst and therefore CO_2 is produced through a parallel mechanism. After that point the curvature changes and becomes convex implying that a different mechanism, comprising series pools, is followed.

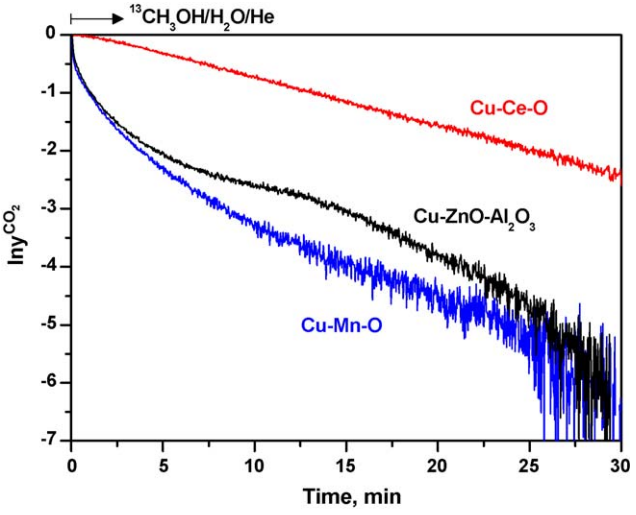

Fig. 3. Semi-logarithmic plot of $\ln(y^{CO_2})$ vs. time after the switch: $^{12}CH_3OH/H_2O/Ar/He \rightarrow {}^{13}CH_3OH/H_2O/He$ over Cu-Ce-O, Cu-Mn-O and Cu-ZnO-Al_2O_3 catalysts at 463 K.

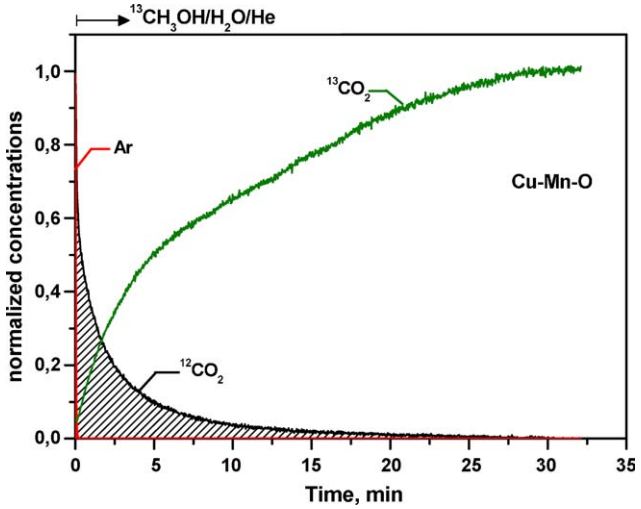

Fig. 4. Normalized responses of Ar and carbon dioxide after the switch: $^{12}CH_3OH/H_2O/Ar/He \rightarrow {}^{13}CH_3OH/H_2O/He$. Cu-Mn-O catalyst at 463 K.

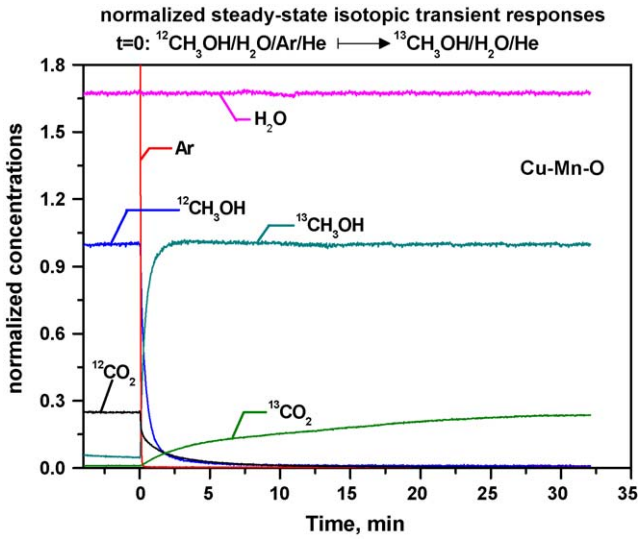

Fig. 5. Normalized response curves of reactants and products according to the gas delivery sequence: $^{12}CH_3OH/H_2O/Ar/He \rightarrow {}^{13}CH_3OH/H_2O/He$. Cu-Mn-O catalyst at 463 K. (all curves normalized with respect to methanol).

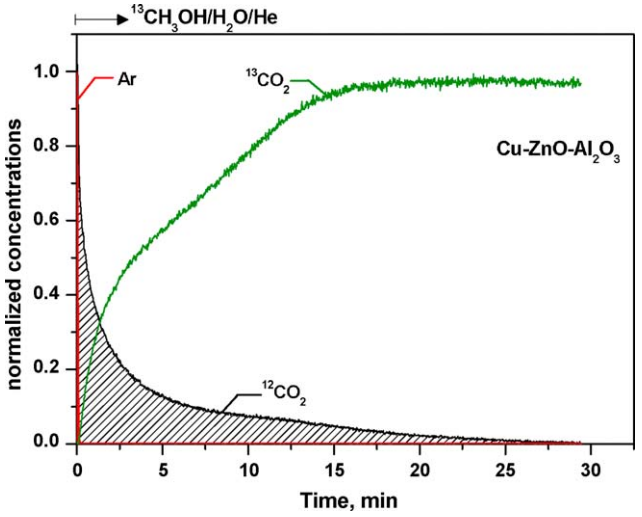

Fig. 6. Normalized responses of Ar and carbon dioxide after the switch: $^{12}CH_3OH/H_2O/Ar/He \rightarrow {}^{13}CH_3OH/H_2O/He$. Cu-ZnO-$Al_2O_3$ catalyst at 463 K.

Table 1 summarizes the results obtained over the three catalysts, during the isotopic switch: $^{12}CH_3OH/H_2O/Ar/He \rightarrow {}^{13}CH_3OH/H_2O/He$. The amounts of adsorbed intermediates are rather comparable over the three catalysts, with Cu-Ce-O showing the lowest value. The Cu-Mn-O catalyst, however, has a higher specific capacity (per unit surface area) by one order of magnitude. On the other hand, the overall mean surface-residence time is more than five times longer over the Cu-Ce-O catalyst compared to Cu-Mn-O and Cu-ZnO-Al_2O_3. Due to this, the reaction rate of CO_2 formation is one order of magnitude smaller over Cu-Ce-O catalyst, as the intermediate species stay longer on its surface.

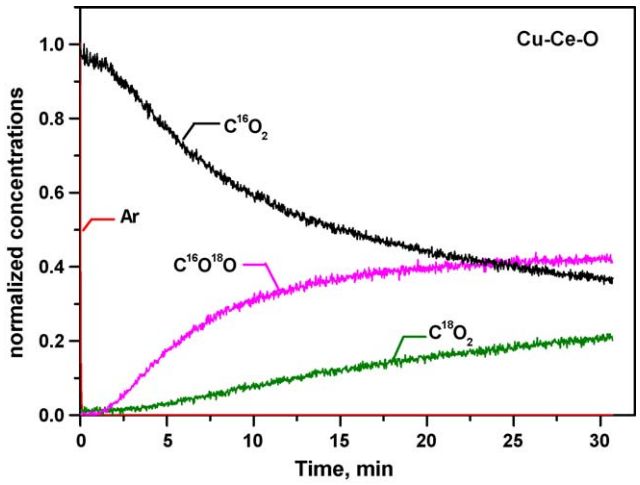

Fig. 7. Normalized curves of Ar and $C^{16}O_2$ disappearance and $C^{16}O^{18}O$ and $C^{18}O_2$ formation after the switch: $CH_3OH/H_2{}^{16}O/Ar/He \rightarrow CH_3OH/H_2{}^{16}O/H_2{}^{18}O/He$. Cu-Ce-O catalyst at 463 K.

3.2. Investigation of "O-path"

Experiments were conducted with the following isotopic switch in the experimental set-up: $CH_3OH/H_2{}^{16}O/Ar/He \rightarrow CH_3OH/H_2{}^{16}O/H_2{}^{18}O/He$. For technical reasons, only 50% of $H_2{}^{16}O$ was substituted by $H_2{}^{18}O$. Fig. 7 presents the transient normalized response curves of $C^{16}O_2$, $C^{16}O^{18}O$, $C^{18}O_2$ and Ar obtained after the isotopic switch over the Cu-Ce-O catalyst. The three responses of the carbon dioxide represent the transient incorporation of ^{18}O atoms from the water, to the intermediate species which contain ^{16}O atoms and lead to the formation of CO_2. Comparing the responses of labeled CO_2 during the switches to labeled H_2O or labeled CH_3OH, it can be observed that these curves have identical shape. Normalized response curves of all reactants and products, in the case of SRM reaction over Cu-Ce-O, are shown in Fig. 8. A very important result in Fig. 8 is the detection of labeled $CH_3{}^{18}OH$ in the products. The presence of ^{18}O in the methanol molecule could be due either to direct exchange of oxygen atoms between water and methanol, or to the reaction mechanism. In order to determine which of the two causes is true, the experiment was also performed at 140 °C, where no methanol conversion takes place. In that case no $CH_3{}^{18}OH$ was formed. This implies that direct exchange of oxygen between the two molecules is excluded as a possibility and, therefore, $CH_3{}^{18}OH$ is produced through one of the intermediate steps of the course of reaction. This will be discussed later on.

Table 1
Overall mean surface-residence time (τ), total amount (N) of adsorbed intermediate species and overall reaction rate (r) under steady-state SRM reaction conditions at 463 K over Cu-Mn-O, Cu-Ce-O and Cu-ZnO-Al_2O_3 catalysts.

Catalyst	$\bar{\tau}^{CO_2}$ (s)	$\bar{N}^{CO_2}$ (μmol g_{cat}^{-1})	$\bar{N}^{CO_2}/S_{BET}$ (μmol m^{-2})	$\bar{r}^{CO_2}$ (μmol g_{cat}^{-1} s^{-1})
Cu-Mn-O[a]	107	361	51.6	3.38
Cu-Ce-O[b]	749	235	5.5	0.31
Cu-ZnO-Al_2O_3[c]	141	386	6.2	2.74

[a] W_{cat} = 9 mg, S_{BET} = 7 m^2 g_{cat}^{-1}, MeOH conversion = 20%.
[b] W_{cat} = 60 mg, S_{BET} = 43 m^2 g_{cat}^{-1}, MeOH conversion = 11.2%.
[c] W_{cat} = 10 mg, S_{BET} = 63 m^2 g_{cat}^{-1}, MeOH conversion = 20%.

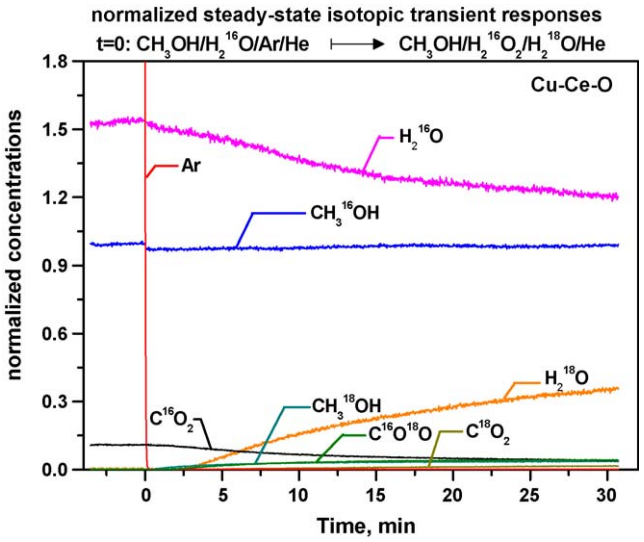

Fig. 8. Normalized response curves of reactants and products of according to the gas delivery sequence: $CH_3OH/H_2{}^{16}O/Ar/He \rightarrow CH_3OH/H_2{}^{16}O/H_2{}^{18}O/He$. Cu-Ce-O catalyst at 463 K (all curves normalized with respect to methanol).

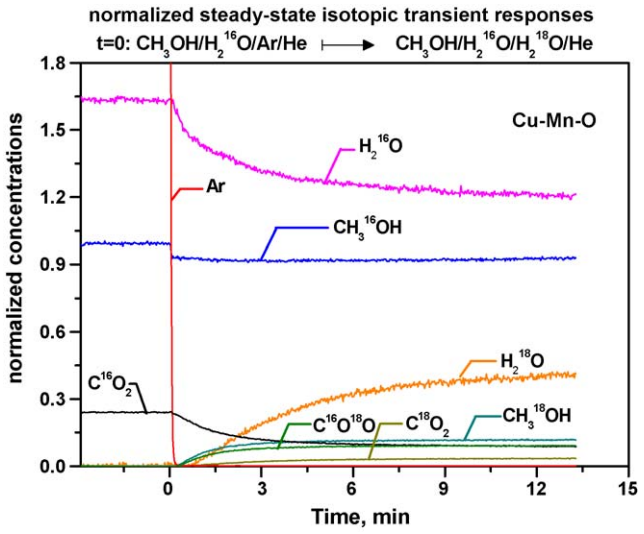

Fig. 10. Normalized response curves of reactants and products according to the gas delivery sequence: $CH_3OH/H_2{}^{16}O/Ar/He \rightarrow CH_3OH/H_2{}^{16}O/H_2{}^{18}O/He$. Cu-Mn-O catalyst at 463 K (all curves normalized with respect to methanol).

Normalized curves of Ar and $C^{16}O_2$ disappearance and $C^{16}O^{18}O$ and $C^{18}O_2$ formation after the switch: $CH_3OH/H_2{}^{16}O/Ar/He \rightarrow CH_3OH/H_2{}^{16}O/H_2{}^{18}O/He$ over the Cu-Mn-O catalyst, are shown in Fig. 9. Carbon dioxide curves are of different shape than the corresponding ones over the Cu-Ce-O catalyst, indicating that different mechanistic routes are followed for the production of CO_2 over these two catalysts. In the case of Cu-Mn-O catalyst, the $C^{16}O_2$ decrease is quicker and so is the production of $C^{16}O^{18}O$ and $C^{18}O_2$. Normalized response curves of both reactants and products according to the aforementioned gas delivery sequence over the Cu-Mn-O catalyst are presented in Fig. 10. All response curves have the same shape, with the increase and decrease of the corresponding MS signals being more abrupt, compared to the ones over the Cu-Ce-O catalyst. A significant amount of ^{18}O-labeled methanol was also observed over the Cu-Mn-O catalyst.

Ar and $C^{16}O_2$ decay response curves as well as the isotopic transient response of $C^{16}O^{18}O$ and $C^{18}O_2$, over the commercial Cu-ZnO-Al_2O_3 catalyst, are presented in Fig. 11. It is worth noting that their shape is alike to the shape of the responses over the Cu-Mn-O catalyst. The normalized response curves of all reactants and products after the switch: $CH_3OH/H_2{}^{16}O/Ar/He \rightarrow CH_3OH/H_2{}^{16}O/H_2{}^{18}O/He$ over the Cu-ZnO-Al_2O_3 catalyst (not shown) were also similar to those observed over the Cu-Mn-O catalyst (Fig. 10). $CH_3{}^{18}OH$ production is again observed, but its concentration is smaller than the one over the other two catalysts tested.

3.3. Reaction mechanism of SRM

The analysis of the C-path in the form of semi-logarithmic plots shows that: (i) the reaction pathway of methanol reforming is a rather complex network consisting of combinations of several parallel and/or consecutive routes and (ii) the fingerprint of each catalyst is different, i.e. specific paths are promoted to a different extent in each catalyst. On the other hand, $CH_3{}^{18}OH$ formation was observed, after switching from $H_2{}^{16}O$ to $H_2{}^{18}O$, over all catalysts tested in this study and, therefore, labeled methanol is produced in

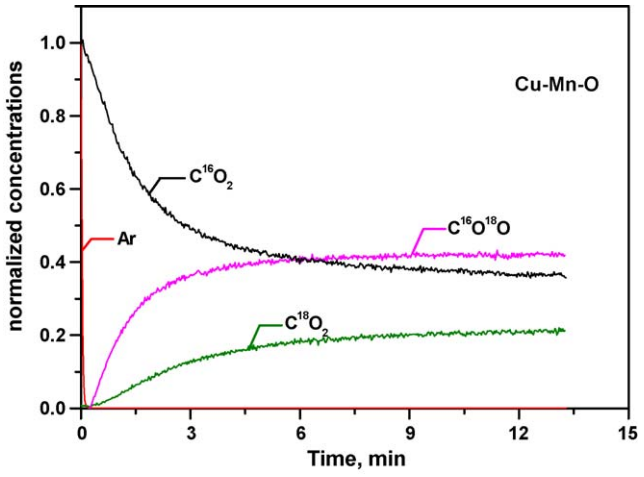

Fig. 9. Normalized curves of Ar and $C^{16}O_2$ disappearance and $C^{16}O^{18}O$ and $C^{18}O_2$ formation after the switch: $CH_3OH/H_2{}^{16}O/Ar/He \rightarrow CH_3OH/H_2{}^{16}O/H_2{}^{18}O/He$. Cu-Mn-O catalyst at 463 K.

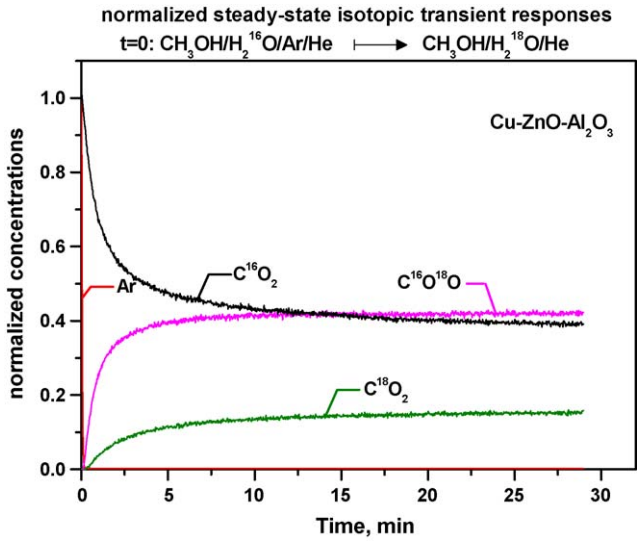

Fig. 11. Normalized curves of Ar and $C^{16}O_2$ disappearance and $C^{16}O^{18}O$ and $C^{18}O_2$ formation after the switch: $CH_3OH/H_2{}^{16}O/Ar/He \rightarrow CH_3OH/H_2{}^{16}O/H_2{}^{18}O/He$. Cu-ZnO-$Al_2O_3$ catalyst at 463 K.

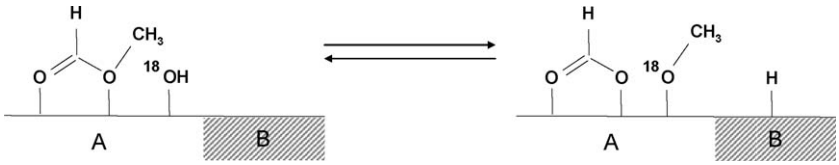

Scheme 1. Elementary step leading to $CH_3{}^{18}OH$ formation.

one of the steps of the SRM reaction. The mechanisms proposed in the literature for the production of hydrogen and carbon dioxide by SRM over Cu-containing catalysts are described below:

(A) Methanol decomposition and WGS

$$CH_3OH \rightarrow CO + 2H_2 \quad (1)$$

$$CO + H_2O \leftrightarrow CO_2 + H_2 \quad (2)$$

(B) Mechanism via methyl formate intermediate

Methanol dehydrogenation to formaldehyde and H_2

$$CH_3OH \rightarrow HCHO + H_2 \quad (3a)$$

$$CH_3OH + HCHO \rightarrow HCOOCH_3 + H_2 \quad (3b)$$

or direct dehydrogenation of methanol to methyl formate and H_2

$$2CH_3OH \rightarrow HCOOCH_3 + 2H_2 \quad (3c)$$

Hydrolysis of methyl formate

$$HCOOCH_3 + H_2O \rightarrow CH_3OH + HCOOH \quad (4)$$

Formic acid decomposition

$$HCOOH \rightarrow H_2 + CO_2 \quad (5)$$

(C) Mechanism via formaldehyde intermediate

Methanol dehydrogenation to formaldehyde

$$CH_3OH \rightarrow HCHO + H_2 \quad (6)$$

Formaldehyde hydrolysis

$$HCHO + H_2O \rightarrow HCOOH + H_2 \quad (7)$$

Formic acid decomposition

$$HCOOH \rightarrow H_2 + CO_2 \quad (8)$$

Mechanism (A) – methanol decomposition followed by WGS – is not considered applicable in the case of Cu-based catalysts, because such catalysts produce CO at concentrations much lower than equilibrium. Mechanism (B), involving a methyl formate intermediate, has been proposed as a possible route over copper catalysts [29,10]. Based on mechanistic studies made by Jiang et al. [30], Peppley et al. [8] and Takezawa and Iwasa [31], Frank et al. [11] presented recently, in a comparative study of copper-containing catalysts, the entire catalytic cycle of methanol steam reforming. The cycle is based on the assumption that the catalytic surface has two distinct types of active sites: one responsible for hydrogen adsorption and the other responsible for the adsorption of all other intermediates. Two different routes are possible following the dissociative adsorption of methanol and its dehydrogenation to formaldehyde: (i) reaction of formaldehyde with adsorbed methoxy species and (ii) reaction of formaldehyde with hydroxyl groups. In the first route, methyl formate is formed as an intermediate, while, in the second route, dioxomethylene is produced. Either one of these two intermediates, decomposes to formate and methanol (methyl formate case) or hydrogen (dioxomethylene case) and afterwards to CO_2 and H_2.

Table 2
Ratio of $CH_3{}^{18}OH$ to CO_2 based on the normalized response curves of $CH_3{}^{18}OH$ and CO_2 obtained during the switch $CH_3OH/H_2{}^{16}O/Ar/He \rightarrow CH_3OH/H_2{}^{16}O/H_2{}^{18}O/He$.

Catalyst	$CH_3{}^{18}OH/CO_2$
Cu-Ce-O	0.34
Cu-Mn-O	0.49
Cu-ZnO-Al_2O_3	0.13

Based on this catalytic cycle, formation of $CH_3{}^{18}OH$ is possible via hydrolysis of methyl formate, as shown below:

$$CH_3{}^{16}OH \rightarrow HCH^{16}O + H_2 \quad (3a)$$

$$CH_3{}^{16}OH + HCH^{16}O \rightarrow HC^{16}O^{16}OCH_3 + H_2 \quad (3b)$$

or

$$2CH_3{}^{16}OH \rightarrow HC^{16}O^{16}OCH_3 + 2H_2 \quad (3c)$$

$$HC^{16}O^{16}OCH_3 + H_2{}^{18}O \rightarrow CH_3{}^{18}OH + HC^{16}O^{16}OH \quad (4)$$

$$HC^{16}O^{16}OH \rightarrow H_2 + C^{16}O_2 \quad (5)$$

$HC^{16}O^{16}O–CH_3$ bond scission takes place in reaction 4 and a new bond is formed between the methyl group and the labeled hydroxyl group originating from labeled water, as shown in Scheme 1. This new ^{18}O-containing methoxy group combines with one adsorbed H and afterwards desorbs as $CH_3{}^{18}OH$. If all $H_2{}^{16}O$ was substituted by $H_2{}^{18}O$, the steady state $CH_3{}^{18}OH$ production should be equal to the total CO_2 concentration, since the stoichiometry between these two is 1:1 (reactions 4 and 5). In the isotopic experiments described above though, only half of $H_2{}^{16}O$ was substituted by $H_2{}^{18}O$. Therefore the amount of $CH_3{}^{18}OH$ should be equal to half of CO_2, since methyl formate has 50% probability to be hydrolyzed by $H_2{}^{16}O$ and 50% to be hydrolyzed by $H_2{}^{18}O$. Table 2 presents the ratios of $CH_3{}^{18}OH$ to the total amount of CO_2, based on their normalized concentrations during the transient $CH_3OH/H_2{}^{16}O/Ar/He \rightarrow CH_3OH/H_2{}^{16}O/H_2{}^{18}O/He$, for the three catalysts tested in the present study. It can be seen that the ratio is almost equal to 0.5 only for the Cu-Mn-O catalyst. Such a result implies that the SRM reaction proceeds mainly via a methyl formate intermediate over Cu-Mn-O.

In the case of Cu-Ce-O, the ratio $CH_3{}^{18}OH/CO_2$ is lower than 0.5. Based on the catalytic cycle of SRM described above, this can be explained assuming that a dioxomethylene intermediate is also present, but to a lesser extend compared to methyl formate. In the case of Cu-ZnO-Al_2O_3 catalyst, whereas the corresponding ratio is much less than 0.5, the SRM reaction should occur mainly via a dioxomethylene intermediate. The conclusions about Cu-Ce-O and Cu-ZnO-Al_2O_3 catalysts are consistent with the results presented in Fig. 3, which indicated a combination of mechanisms for these two catalysts.

4. Conclusions

Cu-Mn-O and Cu-ZnO-Al_2O_3 catalysts show comparable activity in the SRM reaction. This is because they host similar amounts

of adsorbed intermediate species during the course of the reaction and the residence time of adsorbed species on their surface is also similar. The density of active sites is, however, one order of magnitude higher on Cu-Mn-O than on the other two catalysts. The Cu-Ce-O catalyst is one order of magnitude less active, which is mostly due to a lower reactivity of the adsorbed intermediates.

Production of $CH_3{}^{18}OH$ after the switch: $CH_3OH/H_2{}^{16}O/Ar/He \rightarrow CH_3OH/H_2{}^{16}O/H_2{}^{18}O/He$ can be explained by a reaction mechanism involving a methyl formate intermediate. The measured values of the $CH_3{}^{18}OH/CO_2$ ratio indicate that the reaction proceeds almost exclusively via methyl formate hydrolysis over Cu-Mn-O, while via both methyl formate hydrolysis and dioxomethylene dehydrogenation in the case of Cu-Ce-O and Cu-ZnO-Al_2O_3.

References

[1] G. Busca, U. Constantino, F. Marmottini, T. Montanari, P. Patrono, F. Pinzari, G. Ramis, Appl. Catal. A: Gen 310 (2006) 70.
[2] V. Agarwal, S. Patel, K.K. Pant, Appl. Catal. A: Gen. 279 (2005) 155.
[3] J. Papavasiliou, G. Avgouropoulos, T. Ioannides, J. Catal. 251 (2007) 7.
[4] D.R. Palo, R.A. Dagle, J.D. Holladay, Chem. Rev. 107 (2007) 3992.
[5] S. Patel, K.K. Pant, J. Power Sources 159 (2006) 139.
[6] W. Shan, Z. Feng, Z. Li, J. Zhang, W. Shen, C. Li, J. Catal. 228 (2004) 206.
[7] R.O. Idem, N.N. Bakhshi, Chem. Eng. Sci. 51 (1996) 3697.
[8] B.A. Peppley, J.C. Amphlett, L.M. Kearns, R.F. Mann, Appl. Catal. A: Gen. 179 (1999) 31.
[9] J. Agrell, H. Birgersson, M. Boutonnet, J. Power Sources 106 (2002) 249.
[10] M.A. Larrubia Vargas, G. Busca, U. Costantino, F. Marmottini, T. Montanari, P. Patrono, F. Pinzari, G. Ramis, J. Mol. Catal. A: Chem. 266 (2007) 188.
[11] B. Frank, F.C. Jentoft, H. Soerijanto, J. Kröhnert, R. Schlögl, R. Schomäcker, J. Catal. 246 (2007) 177.
[12] R. Burch, A.A. Shestov, J.A. Sullivan, J. Catal. 188 (1999) 69.
[13] K. Tamaru, Appl. Catal. A: Gen. 151 (1997) 167.
[14] Y. Schuurman, C. Mirodatos, Appl. Catal. A: Gen. 151 (1997) 305.
[15] S.L. Shannon, J.G. Goodwin, Appl. Catal. A: Gen. 151 (1997) 3.
[16] S.L. Shannon, J.G. Goodwin, Chem. Rev. 95 (1995) 677.
[17] A.M. Efstathiou, X.E. Verykios, Appl. Catal. A: Gen. 151 (1997) 109.
[18] G.G. Olympiou, Ch.M. Kalamaras, C.D. Zeinalipour-Yazdi, A.M. Efstathiou, Catal. Today 127 (2007) 304.
[19] J.U. Nwalor, J.G. Goodwin, P. Biloen, J. Catal. 117 (1989) 121.
[20] A. Machocki, M. Rotko, B. Stasinska, Catal. Today 137 (2008) 312.
[21] V.A. Tsipouriari, X.E. Verykios, J. Catal. 187 (1999) 85.
[22] S.H. Ali, J.G. Goodwin, J. Catal. 170 (1997) 265.
[23] S.T. Yong, K. Hidajat, S. Kawi, Catal. Today 131 (2008) 188.
[24] J. Papavasiliou, G. Avgouropoulos, T. Ioannides, Catal. Commun. 6 (2005) 497.
[25] J. Papavasiliou, G. Avgouropoulos, T. Ioannides, Catal. Commun. 5 (2004) 231.
[26] W.Y. Suprun, D.P. Sabde, H.-K. Schädlich, B. Kubias, H. Papp, Appl. Catal. A.:Gen. 289 (2005) 66.
[27] A.Ya. Rozovskii, Kinet. Catal. 44 (2003) 391.
[28] H.A.J. van Dijk, J.H.B.J. Hoebink, J.C. Schouten, Chem. Eng. Sci. 56 (2001) 1211.
[29] J.K. Lee, J.B. Ko, D.H. Kim, Appl. Catal. A: Gen. 278 (2004) 25.
[30] C.J. Jiang, D.L. Trimm, M.S. Wainwright, N.W. Cant, Appl. Catal. A: Gen. 97 (1993) 145.
[31] N. Takezawa, N. Iwasa, Catal. Today 36 (1997) 45.